Fluorescent Probes | **Hot Paper**

A Simple Fluorescence Affinity Assay to Decipher Uranyl-Binding to Native Proteins

Fanny Laporte, Yves Chenavier, Alexandra Botz, Christelle Gateau, Colette Lebrun, Sarah Hostachy,* Claude Vidaud, and Pascale Delangle*

Abstract: Determining the affinity of proteins for uranyl is key to understand the toxicity of this cation and to further develop decorporation strategies. However, usual techniques to achieve that goal often require specific equipment and expertise. Here, we propose a simple, efficient, fluorescence-based method to assess the affinity of proteins and peptides for uranyl, at equilibrium and in buffered solution. We first designed and characterized an original uranyl-binding fluorescent probe. We then built a reference scale for uranyl affinity in solution, relying on signal quenching of our fluorescent probe in presence of high-affinity uranyl-binding peptides. We finally validated our approach by re-evaluating the uranyl-binding affinity of four native proteins. We envision that this tool will facilitate the reliable and reproducible assessment of affinities of peptides and proteins for uranyl.

Uranium is the heaviest naturally occurring element, with an estimated abundance of 2–4 ppm in the Earth crust. It is ubiquitous and predominantly present in the environment as the dioxo cation uranyl (UO_2^{2+}), which is radiologically and chemically toxic. Human activities contribute to enrich locally soils and waters in this element. Understanding its interactions with biomolecules, especially proteins, is key to unravel the mechanisms of its toxicity, and to develop strategies for its decorporation. In this process, determining the affinity of a given protein or ligand for uranyl (and its selectivity towards other metal cations) is an important milestone. Various techniques, including SPR, EC-ICP-MS,

CD and Trp fluorescence have been developed to determine affinity constants of proteins.[1–4] However, these techniques are not always suitable for smaller ligands such as peptides or small molecules. In addition, they often require specific equipment and expertise. Experimental conditions, such as pH, buffer composition, ionic strength, etc. may also influence these values. Altogether, this makes the comparison of affinities measured using different experimental conditions and techniques highly delicate.

Therefore, we undertook to develop a method to measure affinities of peptides and proteins for uranyl, at equilibrium and in biologically relevant conditions (aqueous media, physiological pH, etc.). Ideally, such a method should also rely on commonly available techniques and equipment, in order to be easily implemented in chemistry and biochemistry laboratories. Fluorescence spectroscopy was thus the method of choice. Indeed, tryptophan (Trp) fluorescence is already used to measure uranyl binding to proteins. However, proteins do not always bear a Trp, and the presence of multiple Trp or binding sites often complicates model building and data interpretation. We thus sought to design a fluorescent probe that would bind uranyl in aqueous media at pH 7, with a conditional affinity for uranyl similar to endogenous proteins (in the 10^7–10^{12} range), and which signal would not overlap with biological fluorescence.

We showed in the past that short structured peptides can be used as scaffolds to pre-orient metal-chelating groups and obtain high affinity metal ligands, in aqueous buffer and at physiological pH.[5–7] For instance, we reported a series of lanthanide (Ln)-binding hexapeptides **P^{nn}**, incorporating unnatural chelating amino acids Ada$_n$ (Scheme 1). Two

[*] Dr. F. Laporte, Y. Chenavier, Dr. A. Botz, Dr. C. Gateau, C. Lebrun, Dr. S. Hostachy, Dr. P. Delangle
IRIG, SyMMES, Université Grenoble Alpes, CEA, CNRS, Grenoble INP, 38000 Grenoble (France)
E-mail: sarah.hostachy@cea.fr
pascale.delangle@cea.fr

Dr. C. Vidaud
CEA, Fundamental Research Division,
Biosciences and Biotechnologies Institute of Aix-Marseille,
30207 Bagnols sur Céze (France)
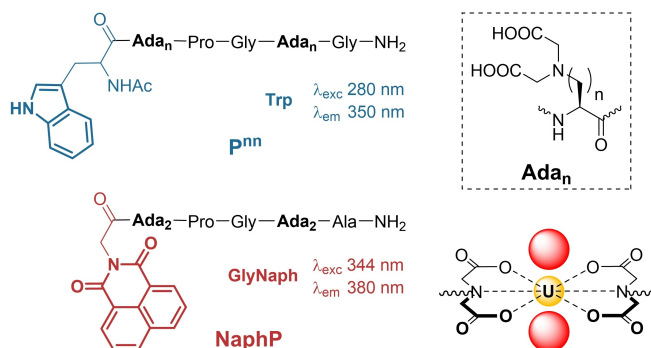
Scheme 1. Sequences of the hexapeptides tested as fluorescent probes for uranyl coordination.

metal-binding amino acids Ada$_n$ were separated by a ProGly sequence to induce a turn, driving the simultaneous coordination of both tridentate iminodiacetate binding groups to Ln ions.[5–7] Like Ln ions, uranyl is a hard ion in the HSAB theory, and favors hard ligands such as carboxylates. However, its linear geometry induces a peculiar coordination, with 4–6 ligands arranged in the plan perpendicular to the O–U–O axis. We therefore reasoned that **P**^{nn} peptides would be good candidates for high affinity uranyl binding. We chose to investigate uranyl coordination by the more constrained scaffolds **P**^{11} and **P**^{22} in priority, since **P**^{33} tended to form polymetallic species with lanthanides.

The conditional equilibrium constant for uranyl complexation was measured using Trp fluorescence quenching upon uranyl addition, following a method previously validated in our team. As previously reported, experiments were performed in presence of excess iminodiacetic acid (IDA), acting as a stabilizing agent avoiding uranyl hydrolysis within the 6 to 7 pH-range, but also as a

competitor for its binding to peptides or proteins.[11] A typical titration is shown in Figure 1A for **P**^{22}. Conditional stability constants for the formation of the UO$_2$**P**^{nn} complexes are reported in Table 1 for three different pH values. Formation of UO$_2$**P**^{nn} complexes was confirmed by ESI-MS at pH 6.9 in ammonium acetate buffer (Figure S1). Mass spectra exhibited signals for uranyl complexes: [UO$_2$+**P**^{22}−4H]$^{2-}$ ($m/z = 577.2$) and [UO$_2$+**P**^{11}−4H]$^{2-}$ ($m/z = 563.2$), as well as small contributions of uranyl-free compounds. Global constants β_{110} were calculated from conditional constants and previously determined pK_a values,[5,6] to compare coordination complex stabilities regardless of ligand acidities, **P**^{11} being significantly less basic that **P**^{22}. The hexapeptide **P**^{22} appeared to be the most efficient uranyl-binding agent, with an affinity for uranyl more than one order of magnitude higher than EDTA.[12] This may be explained by the rather flexible peptide scaffold, that helps accommodating the coordination of the two iminodiacetate groups in the equatorial plane of uranyl. Such a coordination is also found in UO$_2$(IDA)$_2$ complexes[13] and represented in Scheme 1.

Although indicative for simple mixtures, a probe based on Trp quenching would not be suitable for biological samples, since peptides and proteins may contain fluorescent amino acids (like tryptophan, tyrosine or phenylalanine), that could interfere with the probe signal and complicate data analysis. The N-terminal Trp was thus replaced by a non-natural fluorophore, naphthalimide (Naph), which excitation is red-shifted ($\lambda_{exc} = 344$ nm) with respect to natural amino acids ($\lambda_{exc} = 280$ nm). Since **P**^{22} showed the best uranyl-binding properties, this scaffold was chosen for the design of the fluorescent probe **NaphP**. **NaphP** was synthesized by appending the Naph group at the N-terminus of the hexapeptide Gly-Ada$_2$-Pro-Gly-Ada$_2$-Ala on solid support, similarly to a previous report by Bonnet et al.[14] Fluorescence quenching titrations (Figure 1B) demonstrated that **NaphP** behaved similarly to **P**^{22} and had the same affinity for uranyl log$K^{pH\,7} = 9.7$ (Table 1). Most importantly, Naph fluorescence was efficiently quenched by uranyl, with no spectroscopic interference with natural fluorophores. We particularly examined potential interferences with Trp, the most abundant fluorescent amino acid, which is also considered to be the main fluorescence source for excitation at 280 nm and emission at 350 nm.[15,16] For instance, an equimolar solution of the Naph and Trp based peptides showed only the fluorescence of Naph when excited at 344 nm, whereas excitation at 280 nm resulted in emission of both fluorophores (Figure S2 and S3). In summary, **NaphP** exhibited a $10^{9.7}$ affinity for UO$_2^{2+}$ at physiological pH, i.e. in the same range as naturally occurring uranyl-binding proteins, and fluorescence properties orthogonal to those of biological media. It was thus a candidate of choice to probe uranyl binding to proteins in solution at equilibrium and close to physiological conditions.

We reasoned that the uranyl-modulated fluorescence of the probe **NaphP** could be used to build a reference scale for the stability of uranyl complexes. To reach that goal, we exploited a series of cylodecapeptides developed in our group to mimic uranyl binding sites in proteins thanks to
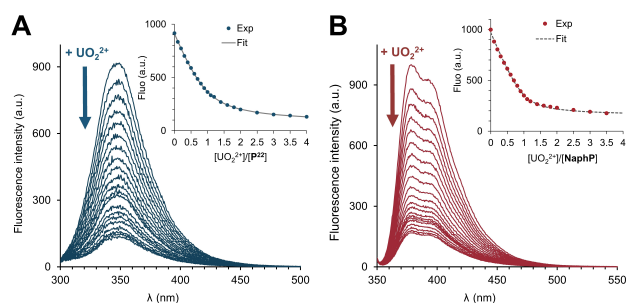

Figure 1. Fluorescence titration following successive addition of UO$_2^{2+}$ (0–4 equiv) to **P**^{22} and **NaphP** in 20 mM HEPES, 0.1 M NaCl buffer at pH 7, in the presence of 10 equiv IDA with respect to probe concentration. *Insets*: variation of the maximum fluorescence intensity following UO$_2^{2+}$ addition. Points represent experimental values and the dotted line corresponds to the best fit obtained with the SPECFIT software.[8–10] The constants of the fit are listed in Table 1. A) **P**^{22} (10 µM), λ_{exc}: 280 nm, λ_{em}: 350 nm; B) **NaphP** (4 µM), λ_{exc}: 344 nm, λ_{em}: 380 nm.

Table 1: Conditional equilibrium constants for the formation of UO$_2$**L** complexes at 25 °C and several pH (Buffer: 20 mM MES, 0.1 M KNO$_3$ at pH 6 and 6.5; 20 mM HEPES, 0.1 M KNO$_3$ at pH 7)[a] and global β_{110} constants calculated from the conditional constants and pK_a values.

L	log$K^{pH\,6}$	log$K^{pH\,6.5}$	log$K^{pH\,7}$	logβ_{110}
P^{11}	8.0(1)	8.5(1)	8.9(1)	9.5(2)[b]
P^{22}	8.0(1)	9.0(1)	9.5(1)	12.8(3)[c]
NaphP			9.7(1)[d]	13.0(1)[c]
EDTA			8.1[e]	11.4[e]

[a] 10 equiv IDA with respect to the ligand were added to the solution and the affinity constants of uranyl with IDA were taken into account in the fitting procedure as previously reported.[11] [b] The pK_a values used to calculate the global β_{110} constant were taken from Ref. [6]. [c] The pK_a values used to calculate the global β_{110} constant were taken from Ref. [5]. [d] 0.1 M NaCl was used to fix the ionic strength to reflect more physiological conditions for the final uranyl fluorescent probe. [e] β_{110} from Ref. [12] at 25 °C and in 0.1 M KNO$_3$. log$K^{pH\,7}$ calculated with the pK_a values found in the same reference.
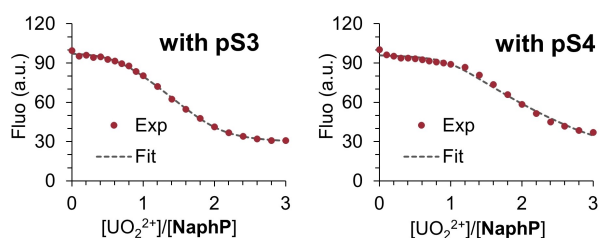
Figure 2. Variation of the maximum fluorescence intensity ($\lambda_{exc} = 344$ nm, $\lambda_{em} = 380$ nm) of a solution of **NaphP** (2 μM) in presence of 2 μM **pS3** (left) or **pS4** (right), following UO_2^{2+} addition. Dots are experimental values and dashed lines represent the best fits obtained with SPECFIT software, with the following constants:10.9, 17.0 and 19.2 for **pS3** and 11.5, 16.4 and 21.0 for **pS4**, for the complexes $UO_2\textbf{pSn}$, $UO_2(\textbf{pSn})_2$ and $(UO_2)_2\textbf{pSn}$, respectively.[8–10]
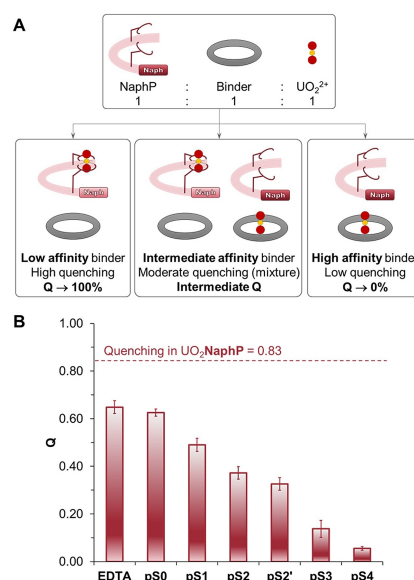

Figure 3. A) Principle of the affinity assay. B) Fluorescence quenching of the probe **NaphP** upon addition of EDTA or a biomimetic peptide, followed by uranyl addition, in equimolar concentrations and in buffered conditions (20 mM HEPES pH 7, 100 mM NaCl, 25 °C). [**NaphP**] = [EDTA or peptide] = [UO_2^{2+}] = 2 μM.

four coordinating glutamate and/or phosphoserine (pSer) residues.[11,17–19] These peptides were named **pSn**, n being the number of pSer and (4−n) being accordingly the number of coordinating glutamates in the sequence. Sequences of the peptides used in this study are described in the Supporting Information (Table S1). We recently demonstrated that uranyl-binding affinity significantly increased along with n, as shown by the conditional stability constants at pH 7 (Table 2). In our previous study, both phosphate-rich peptides **pS3** and **pS4** showed a quite complicated speciation, with three uranyl complexes formed during the titration with uranyl, namely $UO_2\textbf{pSn}$, $UO_2(\textbf{pSn})_2$ and $(UO_2)_2\textbf{pSn}$. As a consequence, analysis of the Trp fluorescence data had been performed making assumptions on the emitting or non-emitting character of these metal species.[17] It was thus necessary to confirm the obtained stability constants prior to building an affinity scale. **NaphP** fluorescence being independent from the fluorescence of the $UO_2\textbf{pSn}$ complexes, it was possible to re-assess these constants by observing Naph fluorescence ($\lambda_{ex} = 344$ nm, $\lambda_{em} = 380$ nm). In experiments where **NaphP** and either **pS3** or **pS4** competes for UO_2^{2+} binding (Figure 2), Naph fluorescence signal remained stable at the beginning of each titration, indicating that affinities of both phosphate-rich peptides for uranyl were significantly larger than that of the probe. The fit of the overall Naph fluorescence evolution pointed to the formation of the three above-mentioned complexes, as in our previous analysis (Table S2). Importantly, constants found for the 1:1 $UO_2\textbf{pSn}$ complexes were particularly large, and consistent with previous determination: $10^{10.9}$ and $10^{11.5}$ for **pS3** and **pS4**, respectively.[17]

Having confirmed the stability constants, it was then possible to build the affinity scale. Quenching of **NaphP** probe by uranyl was defined as $Q = (F_0 - F_U)/F_0$, F_0 and F_U being the fluorescence intensities at 380 nm for excitation at 344 nm, before and after uranyl addition, respectively. Q was chosen as readout for the affinity scale. Equimolar concentrations of uranyl, probe and peptide were used, so that uranyl would be the limiting factor and distribute between the probe and the peptide according to their relative affinities, forming 1:1 complexes. If the peptide affinity for uranyl was high, then only little $UO_2\textbf{NaphP}$

complex would form and the probe would mainly be present as free, emissive **NaphP**, leading to little quenching as compared to uranyl-free conditions. So, the higher the affinity of the peptide, the lower Q. (Figure 3). We measured Q in presence of biomimetic peptides **pSn** or the simple low affinity ligand EDTA, at pH 7 and at equilibrium, with equimolar mixtures of probe, peptide and uranyl.

As expected, EDTA and **pS0** induced relatively high Q, indicating significantly lower affinities for uranyl than **NaphP**, whereas phosphorylated peptides **pSn** ($n > 0$) notably decreased the signal-quenching of the probe, due to part of the metal coordinated to the biomimetic peptide. As n increased, Q decreased, which is consistent with the higher affinities of the more phosphorylated peptides for uranyl. Significantly, the quantity of $UO_2\textbf{NaphP}$ complex determined experimentally from fluorescence quenching correlated well with the quantity calculated from known stability constants (Figure S4). Most importantly, conditional stability constants of 1:1 uranyl complexes for the series of biomimetic peptides and EDTA decreased linearly as the fluorescence quenching Q of the probe **NaphP** increased (Figure 4). This confirms that the measurement of **NaphP** quenching can be used to access stability data for unknown compounds, provided it is within the range of the affinity scale. Note that, to get reliable affinity constants, this assay should be performed in controlled conditions, and in absence of competing metals.

Using this affinity scale, the uranyl-binding affinities of four native uranyl target proteins (serum albumin, apo-transferrin, fetuin-A and osteopontin) could then be easily evaluated by measuring the quenching Q at equilibrium in solution, following the same procedure.

Table 2: Conditional equilibrium constants for the formation of UO$_2$**pSn** complexes at 25 °C and pH 7 (20 mM HEPES, 0.1 M NaCl) for the series of biomimetic cyclodecapeptides.

pSn	pS0[11]	pS1[19]	pS2[18]	pS2′[18]	pS3	pS4
log $K^{pH\,7}$	8.2(1)	9.1(1)	10.1(1)	9.7(1)	10.9(1)	11.5(1)
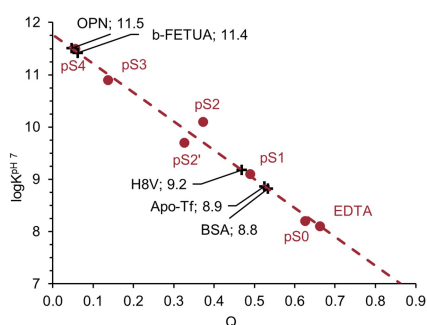
Figure 4. Correlation of the affinity constants expressed as log $K^{pH\,7}$ for the UO$_2$P complexes with Q, the fluorescence quenching of the **NaphP** probe. Conditions: [**NaphP**] = [EDTA or peptide] = [UO$_2^{2+}$] = 2 μM. 20 mM HEPES pH 7, 100 mM NaCl at 25 °C: Red points and linear regression (dotted red line, R^2 = 0.97). Black crosses: experimental Q for 4 uranyl-binding proteins and the short peptide sequence **H8V** selected from OPN and equilibrium constants of the corresponding 1:1 UO$_2^{2+}$ complexes calculated from the regression.

Serum albumin (HSA and BSA for Human and Bovine serum albumin, respectively) and apo-transferrin (apo-Tf) were believed to be the main targets of uranyl in serum for a long time.[20,21] However, literature shows large discrepancies in the corresponding equilibrium constants, depending on which experimental conditions and methods were used. For instance, microcalorimetry experiments showed two uranyl binding sites for BSA at pH 5.5, with log K = 7.2 and 5.4.[22] Using fluorescence quenching of the proteins, log K = 6.1 and 7.7 were obtained at pH 7.4 for HSA and Apo-Tf, respectively, although without controlling the formation of hydroxo uranyl complexes.[23] Time-resolved laser-induced fluorescence spectroscopy experiments determined stability constants log K = 10.8 for HSA and 11.4–12.4 for apo-Tf at pH 7.4, with huge variations upon presence of carbonate.[24] Strikingly, both proteins gave significant quenching values in our assay (close to 50%), indicating similar, moderate stability constants: log $K^{pH\,7}$ = 8.8 and 8.9 for BSA and apo-Tf, respectively (Figure 4).

Bovine fetuin-A (b-FETUA), a serum protein,[25] and osteopontin (OPN), a protein involved in bone turnover,[3] were identified more recently as having some of the largest affinities for the uranyl ion. Indeed, in presence of these proteins, nearly no quenching of the probe luminescence could be observed (Q = 6% and 5% respectively, see Figure 4), indicating that the protein bound almost all uranyl ions present in the assay. These quenching values were close to those measured with the biomimetic peptide **pS4** (Q = 6%), resulting in similar log $K^{pH\,7}$ (11.4 and 11.5 for b-FETUA and OPN, respectively). This is in line with reported affinities from CE-ICP-MS experiments, that gave exactly the same values for both proteins.[2,26] The latter

value was obtained making the assumption of a ternary complex b-FETUA–UO$_2$–CO$_3$ formed at low carbonate content. Hence, the present analysis corroborated these assumptions and confirmed the outstanding affinities of these two native proteins for uranyl.

We also investigated the short synthetic peptide **H8V**, pSDEpSDE, selected from OPN sequence and containing two phosphorylated serine (pSer) residues.[27] Interestingly, **H8V** gave a quenching similar to the model peptide **pS1**, which coordinates uranyl with three carboxylates and only one phosphate (Figure 4). This is consistent with structural data acquired for **H8V**, showing coordination of only one phosphate.[27] Using the affinity scale, affinity of **H8V** for UO$_2^{2+}$ was extrapolated to log K = 9.2. This value is significantly lower than those obtained for the cyclic biomimetic peptides **pS2** and **pS2′**, although they also contain two pSer residues. In these latter peptides, pre-orientation of the amino acid side chains favors coordination to the metal cation. The fluorescence quenching method with **NaphP** was demonstrated here to be highly sensitive to the affinity constant.

In this work, we designed and characterized an original uranyl-binding fluorescent probe, based on a peptide rigid-turn structure that pre-oriented two unnatural amino acid side chains to efficiently coordinate uranyl. Two iminodiacetic moieties could thus be accommodated in the equatorial plane of uranyl at physiological pH, with an affinity in the range of those of native proteins. Importantly, incorporation of a naphthalimide fluorophore enables the detection of uranyl binding with emission properties orthogonal to biological media, thereby eliminating interferences with naturally occurring fluorophores. Using a series of previously reported high-affinity uranyl-binding peptides, we then built a reference scale for uranyl affinity in solution, relying on signal quenching of our fluorescent probe. We could show that there was a linear correlation between log K and fluorescence quenching Q, making extrapolation to other proteins and peptides straightforward. We finally validated our approach by re-evaluating the uranyl-binding affinity of four native proteins, confirming unambiguously that b-Fetuin and OPN have significantly larger affinities for uranyl than more abundant serum proteins BSA and Apo-Tf. Unlike other techniques, this affinity assay was easy to implement with common laboratory equipment (a fluorimeter) and did not necessitate advanced technical expertise. In addition, measurements could be performed in solution, in physiological conditions, and required only limited amounts of samples. We thus envision that this tool will facilitate the reliable and reproducible assessment of affinity of peptides and proteins for uranyl.

Conflict of Interest

The authors declare no conflict of interest.

Data Availability Statement

The data that support the findings of this study are available from the corresponding author upon reasonable request.

[1] O. Averseng, A. Hagège, F. Taran, C. Vidaud, *Anal. Chem.* **2010**, *82*, 9797–9802.

[2] T.-N. S. Huynh, D. Bourgeois, C. Basset, C. Vidaud, A. Hagège, *Electrophoresis* **2015**, *36*, 1374–1382.

[3] L. Qi, C. Basset, O. Averseng, E. Quéméneur, A. Hagège, C. Vidaud, *Metallomics* **2014**, *6*, 166–176.

[4] H. Zänker, K. Heine, S. Weiss, V. Brendler, R. Husar, G. Bernhard, K. Gloe, T. Henle, A. Barkleit, *Inorg. Chem.* **2019**, *58*, 4173–4189.

[5] F. Cisnetti, C. Gateau, C. Lebrun, P. Delangle, *Chem. Eur. J.* **2009**, *15*, 7456–7469.

[6] F. Cisnetti, C. Lebrun, P. Delangle, *Dalton Trans.* **2010**, *39*, 3560–3562.

[7] L. Ancel, C. Gateau, C. Lebrun, P. Delangle, *Inorg. Chem.* **2013**, *52*, 552–554.

[8] H. Gampp, M. Maeder, C. J. Meyer, A. D. Zuberbühler, *Talanta* **1985**, *32*, 95–101.

[9] H. Gampp, M. Maeder, C. J. Meyer, A. D. Zuberbühler, *Talanta* **1985**, *32*, 257–264.

[10] H. Gampp, M. Maeder, C. J. Meyer, A. D. Zuberbühler, *Talanta* **1985**, *32*, 1133–1139.

[11] C. Lebrun, M. Starck, V. Gathu, Y. Chenavier, P. Delangle, *Chem. Eur. J.* **2014**, *20*, 16566–16573.

[12] P. A. Overvoll, W. Lund, *Anal. Chim. Acta* **1982**, *143*, 153–161.

[13] J. Jiang, M. J. Sarsfield, J. C. Renshaw, F. R. Livens, D. Collison, J. M. Charnock, M. Helliwell, H. Eccles, *Inorg. Chem.* **2002**, *41*, 2799–2806.

[14] C. S. Bonnet, M. Devocelle, T. Gunnlaugsson, *Chem. Commun.* **2008**, 4552–4554.

[15] F. W. J. Teale, G. Weber, *Biochem. J.* **1957**, *65*, 476–482.

[16] A. Ghisaidoobe, S. Chung, *Int. J. Mol. Sci.* **2014**, *15*, 22518–22538.

[17] F. A. Laporte, C. Lebrun, C. Vidaud, P. Delangle, *Chem. Eur. J.* **2019**, *25*, 8570–8578.

[18] M. Starck, N. Sisommay, F. A. Laporte, S. Oros, C. Lebrun, P. Delangle, *Inorg. Chem.* **2015**, *54*, 11557–11562.

[19] M. Starck, F. A. Laporte, S. Oros, N. Sisommay, V. Gathu, P. L. Solari, G. Creff, J. Roques, C. Den Auwer, C. Lebrun, P. Delangle, *Chem. Eur. J.* **2017**, *23*, 5281–5290.

[20] E. Ansoborlo, O. Prat, P. Moisy, C. Den Auwer, P. Guilbaud, M. Carriere, B. Gouget, J. Duffield, D. Doizi, T. Vercouter, C. Moulin, V. Moulin, *Biochimie* **2006**, *88*, 1605–1618.

[21] P. W. Durbin in *The Chemistry of the Actinide and Transactinide Elements* (Ed.: L. R. Morss, N. M. Edelstein, J. Fuger), Springer Netherlands, Dordrecht, **2006**, pp. 3339–3440.

[22] M. R. Duff, C. V. Kumar, *Angew. Chem. Int. Ed.* **2006**, *45*, 137–139; *Angew. Chem.* **2006**, *118*, 143–145.

[23] J. Michon, S. Frelon, C. Garnier, F. Coppin, *J. Fluoresc.* **2010**, *20*, 581–590.

[24] G. Montavon, C. Apostolidis, F. Bruchertseifer, U. Repinc, A. Morgenstern, *J. Inorg. Biochem.* **2009**, *103*, 1609–1616.

[25] C. Basset, O. Averseng, P.-J. Ferron, N. Richaud, A. Hagège, O. Pible, C. Vidaud, *Chem. Res. Toxicol.* **2013**, *26*, 645–653.

[26] T.-N. S. Huynh, C. Vidaud, A. Hagège, *Metallomics* **2016**, *8*, 1185–1192.

[27] S. Safi, G. Creff, A. Jeanson, L. Qi, C. Basset, J. Roques, P. L. Solari, E. Simoni, C. Vidaud, C. Den Auwer, *Chem. Eur. J.* **2013**, *19*, 11261–11269.